Journal of Catalysis **202,** 156–162 (2001)
doi:10.1006/jcat.2001.3279, available online at http://www.idealibrary.com on IDEAL®

Selective Catalytic Reduction of Nitrous Oxide by Ammonia on Iron Zeolite Beta Catalysts in an Oxygen Rich Atmosphere: Effect of Iron Contents

G. Delahay,*[,1] M. Mauvezin,* B. Coq,* and S. Kieger†

*Laboratoire de Matériaux Catalytiques et Catalyse en Chimie Organique, UMR CNRS-ENSCM 5618, ENSCM, 8 rue d l'Ecole Normale, 34296 Montpellier Cedex 5, France; and †Grande Paroisse, 12 place de l'Iris, 92062 Paris-La Défense Cedex, France

Received February 16, 2001; revised May 14, 2001; accepted May 17, 2001

A series of iron-exchanged zeolite beta (BEA) has been characterized by temperature programmed desorption (TPD) of oxygen and tested in the catalytic reduction of N_2O by NH_3. TPD of O_2 has clearly shown that iron-oxo species formed upon reoxidation by nitrous oxide of Fe^{2+}-BEA are more labile than those generated by calcination in air. In the selective catalytic reduction of N_2O by NH_3 the conversion of N_2O increases until a degree of iron exchange level of 100% and then decreases. In contrast, the intrinsic activity per mole of iron decreases drastically with the increase of iron content. Mononuclear iron-oxo species have been proposed as the most active sites for the reduction of N_2O by NH_3; binuclear iron-oxo species and iron oxides aggregates are less active. © 2001 Academic Press

Key Words: **nitrous oxide; ammonia; iron; zeolite; selective reduction; temperature programmed desorption.**

INTRODUCTION

In recent years iron-exchanged zeolites (Fe-Z) have received increasing attention as catalytic materials for the $deNO_x$ catalysis (1–8). In this context new preparations of Fe-ZSM-5 catalysts have been led to catalysts with high activity and stability in the selective catalytic reduction (SCR) of NO_x by hydrocarbons (1, 2, 4) or by NH_3 (7, 8). The removal of nitrous oxide (deN_2O) by efficient catalytic methods is also a subject of topical interest with regard to protecting the environment (9). N_2O is classified as a non-CO_2 greenhouse gas that contributes to the catalytic depletion of the stratospheric ozone layer. The simplest control technology for N_2O removal is based on its catalytic decomposition to N_2 and O_2 (10). The slow-step, desorption of surface oxygen can be facilitated by addition of a selective reductant such as a hydrocarbon, ammonia, or carbon monoxide (11–15). We have recently shown (16) that ammonia clearly improves the decomposition of N_2O to N_2 in the presence of oxygen over iron-exchanged zeolites. On a Fe-zeolite-beta (Fe-BEA, 0.9 wt%), and with a space velocity of 30,000 h^{-1}, the light-off temperature in the reduction of N_2O by NH_3 (50% N_2O conversion) occurs at 665 K, which is 80 K lower than the catalytic decomposition of N_2O (16). However, the same study showed that Fe-zeolite materials exhibited very different behavior depending on the nature of the zeolite, which likely affects the nature of the Fe species.

Yamada *et al.* (15) and Pophal *et al.* (17) have shown in the SCR of N_2O by propene on Fe-ZSM-5 that the conversion of N_2O increases linearly with the iron exchange level, and thus the turnover frequency (TOF = mole of N_2O converted per mole of iron and per hour) remains more or less constant. Such behavior could indicate that the nature of Fe species remains similar whatever the exchange level.

In the oxidation of methane and benzene by N_2O, the activity of [Fe]-ZSM-5 was postulated to be linked to the presence of an extra lattice iron species and, more precisely, to binuclear iron-oxo complexes (18–20). More generally, binuclear iron complexes with different oxo-, hydroxo-, or peroxo- coordination of oxygen around iron are suggested to be the active sites in the reduction of nitrogen oxides over Fe-zeolites (21–24). Joyner and Stockenhuber (3) have shown by XAFS the presence of two different iron species: mononuclear ions and oxo nanoclusters (Fe_4O_4) in ZSM-5. The distribution of these species varies with preparation method and the nature of the pretreatment. They attributed the high activity of Fe-ZSM-5 in the SCR of NO by propene to these small Fe_4O_4 clusters. We have recently shown that iron-oxo species are mainly present in the Fe-BEA catalysts prepared from the conventional exchange procedure (25). Binuclear oxo cations are formed after activation in air, whereas activation in N_2O of the prereduced Fe-BEA leads to both mono- and binuclear oxo cations; the former are favored at low exchange level. These observations prompted us to speculate that the reactivity of Fe-BEA should thus depend on the Fe content.

Therefore, this study addresses the effect of the degree of iron exchange level on the catalytic behavior of Fe-BEA in the SCR of N_2O by ammonia in the presence of oxygen and seeks to determine the nature of the iron active species.

---

[1] To whom correspondence should be addressed. Fax: +33 (0)4 67 14 43 49. E-mail: delayhay@cit.enscm.fr.

0021-9517/01 $35.00

EXPERIMENTAL

Preparation of the Catalysts

Depending on the metal loading chosen, different methods were carried out for the preparation of Fe(x)BEA, with x being the theoretical degree of exchange ($x = 300$Fe/Al, mol/mol). The chemicals used were H-BEA zeolite (PQ corporation zeolite CBV 810B-25, specific surface area = 680 $m^2\ g^{-1}$, Si/Al = 12.5) and $Fe(NO_3)_3$, $9H_2O$ (Aldrich, 98 + %).

The samples of low exchange levels ($x < 100$) were prepared by an ion-exchange method and called Fe(x)BEAe. H-BEA (2 g) was added to 500 cm^3 of a $Fe(NO_3)_3$ aqueous solution [(0.5–2) $\times 10^{-3}$ mol L^{-1}] and then stirred for 48 h; the pH of the slurry was kept at 3.8–4.0 by adding diluted NH_4OH solution. After filtration the solid was washed three times before being dried at 353 K in air.

Heavily loaded Fe(126)BEAi, Fe(169)BEAi, and Fe(375)BEAi were prepared by dry impregnation. H-BEA (2 g) was poured in 10 cm^3 of a $Fe(NO_3)_3$ aqueous solution; after evaporation the solid was dried at 353 K in air.

A 8.5% Fe_2O_3/BEA sample was obtained as a mechanical mixture of 17 mg Fe_2O_3 (Prolabo) with 184 mg H-BEA.

The chemical analyses of the materials were performed using plasma atomic absorption spectroscopy at the Service Central d'Analyse du CNRS (Vernaison, France) and are reported in Table 1.

Temperature Programmed Desorption of O_2(O_2-TPD)

O_2-TPD experiments of the calcined samples were carried out with a Micromeritics 2910 apparatus coupled at a quadruple mass spectrometer (Pfeiffer Omnistar) equipped with Channeltron and Faraday detectors (0–200 amu). The carrier gas was helium (flow rate = 10 $cm^3\ min^{-1}$ NTP) and the heating ramp was 30 K min^{-1} from 293 to 1073 K. The sample (200 mg) was first calcined in air (O_2/N_2: 20/80) for 2 h at 823 K or activated in N_2O/He before analysis. In the case of activation in N_2O/He, the sample was first reduced for 2 h at 973 K in H_2/Ar (3/97). After cooling to room temperature in H_2/Ar, the sample was then activated in N_2O/He (5/95) at 973 K for 2 h and then cooled to 353 K in the same gas.

N_2O Decomposition and SCR of N_2O by NH_3

The N_2O decomposition and the SCR of N_2O by NH_3 were studied in a flow reactor operating at atmospheric pressure. Catalyst aliquots (≈100 mg) were activated *in situ* at 823 K in air (O_2/N_2: 20/80) for 2 h (ramp = 10 K min^{-1}, flow rate = 50 $cm^3\ min^{-1}$ NTP) and then cooled to room temperature. The reaction gas, a mixture of N_2O/O_2/He (0.2/3.0/96.8) and $N_2O/O_2/NH_3$/He (0.2/3.0/0.2/96.6) for the decomposition and the SCR of N_2O, respectively, was fed to the catalyst. The space velocity was 35,000 h^{-1}. The catalytic tests were carried out in temperature programmed surface reaction (TPSR) from 298 to 823 K at 5 K min^{-1}. The effluent composition was monitored continuously by sampling online to a quadruple mass spectrometer (Pfeiffer Omnistar) equipped with Channeltron and Faraday detectors (0–200 amu). Nine masses characteristic of NO (*30*), NO_2 (30, *46*), N_2O (28, 30, *44*), N_2 (*28*), NH_3 (*17*, 18), H_2O (17, *18*), O_2 (16, *32*), and He (*4*) were followed. The intensities of NH_3 (17), H_2O (18), N_2 (28), and NO (30) were determined by solving a linear system of equations. The concentrations were derived from intensities by using standardization procedures before and after each experiment.

TABLE 1

Some Characteristics of Fe-BEA Samples at Different Fe Loadings

Sample	Si/Al (mol/mol)	Fe/Al (mol/mol)	Theoretical exchange degree (%)	Specific surface area[a] ($m^2\ g^{-1}$)	H_2/TPR[b] H_2/Fe[c] (mol/mol)	H_2/TPR[b] H_2/Fe[d] (mol/mol)
Fe(6)BEAe	13.1	0.020	6	615		
Fe(10)BEAe	12.7	0.035	10	618		
Fe(24)BEAe	13.7	0.079	24	614	0.25	1.00
Fe(49)BEAe	12.8	0.164	49	609	0.32	0.60
Fe(79)BEAe	12.1	0.263	79	605		0.70
Fe(97)BEAe	13.3	0.323	97	600	0.42	0.26
Fe(126)BEAi	11.9	0.420	126	583	0.46	0.49
Fe(169)BEAi	11.5	0.562	169	587	0.44	
Fe(375)BEAi	14.2	1.250	375	530	0.88	0.53

[a] For a sake of simple comparison between the samples, the specific surface area was determined according to the BET method, even if this method has no physical meaning for N_2 adsorption in microporous zeolites.

[b] TPR by H_2/Ar (3/97) with a ramp of 10 K/min between 353 K and 973 K (from Ref. 25).

[c] Samples calcined in air at 823 K.

[d] Samples reduced by H_2/Ar (3/97) at 973 K for 2 h and, after cooling to room temperature, then activated in N_2O/He (5/95) at 973 K for 2 h.

RESULTS

O_2-*TPD*

Samples calcined in air at 823 K. Figure 1 shows the O_2-TPD profiles of the different samples pretreated in air at 823 K. H-BEA and Fe_2O_3/BEA do not desorb any significant amount of oxygen. For the other solids O_2 starts to desorb above 723 K with a maximum occurring around 1020 K. The total amount of oxygen desorbing from the sample greatly increases with the exchange level up to the theoretical total exchange of 100% and then decreases. It should be noticed that for Fe(10)-BEAe uncertainty on the measure is very important due to the very weak quantity of desorbed oxygen per gram of solid (Fig. 2). Moreover, for Fe(6)-BEA none of the measures could be made with sufficient accuracy. In contrast, the molar ratio O_2/Fe increases with the decrease of iron content in the sample (Fig. 2) and reaches a value of 0.35 for Fe(24)BEAe.

Samples reduced by H_2(H_2/Ar, 3/97) at 973 K and reoxidized by O_2 (O_2/He, 3/97) at 823 K. A mild reduction in H_2/Ar (3/97) leads to the reduction of Fe^{3+} to Fe^{2+} cations (24–27). As an example, the O_2-TPD profile of Fe(97)-BEAe, reduced in H_2/Ar (3/97) and then reoxidized in O_2/He (3/97) at 823 K, is shown in Fig. 1f. Oxygen desorbs in the same temperature range but the amount is much lower than that occuring after calcination in air. One can therefore speculate that O_2/He (3/97) is unable to restore the same amount of O_2 species that calcination in air can. Similar results were obtained for the other Fe(x)-BEA catalysts.

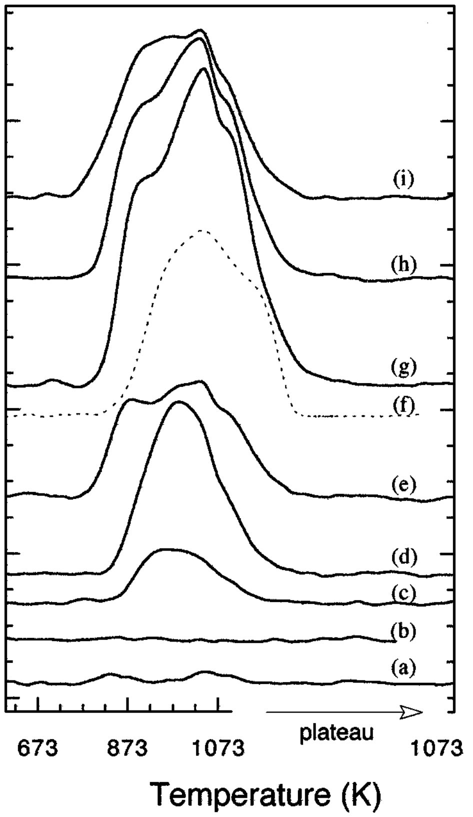

FIG. 1. O_2-TPD profiles of calcined materials in air (full lines) and in 3%O_2/He (dotted lines): (a) H-BEA, (b) 8.5%Fe_2O_3/BEA, (c) Fe(10)BEAe, (d) Fe(24)BEAe, (e) Fe(49)BEAe, (f) Fe(97)BEAe, (g) Fe(97)BEAe, (h) Fe(126)BEAi, (i) Fe(375)BEAi; conditions: carrier gas = helium, 10 K min^{-1}.

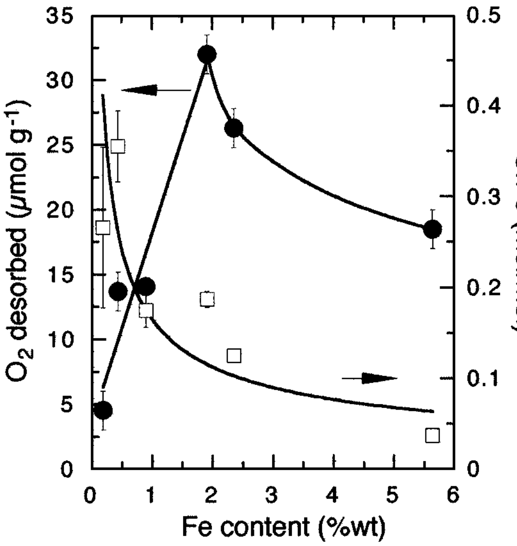

FIG. 2. Amount of O_2 desorbed from Fe-BEA as a function of Fe content, during the O_2-TPD (data from Fig. 1).

Samples reduced by H_2 (H_2/Ar, 3/97) at 973 K and reoxidized by N_2O (N_2O/He, 5/95) at 973 K. After treatment of the reduced samples by N_2O/He (5/95), three broad massifs composed of unresolved peaks appear in the O_2-TPD profiles followed by both katharometric and mass spectrometry detection (Fig. 3). One should note that after activation at 973 K in N_2O/He, the sample was cooled to room temperature in the same gas. An example of an O_2-TPD profile is given in Fig. 3a for the typical case of Fe(97)BEAe. The nature of desorbing species was identified by mass spectroscopy; desorption peaks corresponded to N_2O at 450 K and to NO at ca 670 K, and three peaks of O_2 desorption were at 610, 790, and 940 K. It clearly appears that a different surface oxygen exists after N_2O treatment because O_2 desorbs significantly more at low temperature ($\approx$610 K) compared to samples calcined with O_2/He (3/97) or air. In contrast, if before N_2O treatment the sample was calcined but not reduced, the amount of O_2 desorbing at low temperature was much smaller (Fig. 3a). The weakly bound O_2 species desorbing at low temperature are thus specifically formed by interaction of N_2O with reduced Fe sites. These surface O^* species are also very easily removed by H_2 and CO (below 500 K), as TPR experiments have shown

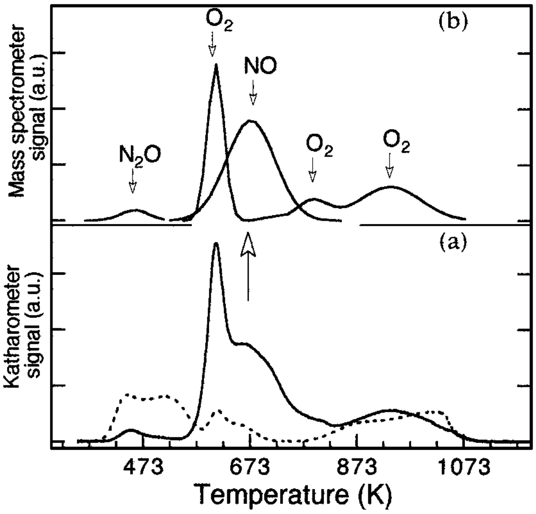

FIG. 3. O_2-TPD profiles of Fe(97)BEAe from (a) katharometric detection and (b) mass spectrometry detection: (dotted lines) after treatment by N_2O of the calcined sample; (full lines) after treatment by N_2O of the prereduced sample by H_2/Ar (3/97). Conditions: carrier gas = helium, 10 K min^{-1}.

(25). It is obvious that NO formation comes from the N–NO splitting on the reduced sample. N–NO splitting was proposed to account for the presence in certain conditions of $^{14}N^{15}N$ in the reduction of $^{14}N_2O$ by $^{15}NH_3$ (12). N–NO splitting was also recently proposed from the interaction of N_2O with Fe(II) species in Fe-ZSM-5 and Fe-MCM-41 (28, 29).

For the various samples, we have plotted in Fig. 4 the molar ratio O/Fe of O_2 desorbing in the low temperature ($LT < 700$ K) and high temperature ($HT > 700$ K) domains, depending on the pretreatment. The O/Fe molar ratio at HT is independent of the pretreatment, whereas there is a significant O_2 desorption at LT only after N_2O treatment of the reduced sample, with a strong increase of O/Fe value when the Fe content decreases.

Catalytic Experiments

Several catalytic tests were carried out in the SCR of N_2O to identify the occurrence of any pore diffusion limitation. They were conducted in steady state conditions at 613 K by using sieved fractions from 0.12 to 0.4 mm of Fe(97)BEAe, the most active catalyst. No differences appeared in the N_2O conversion, which provides evidence that the intraparticle mass transfer is fast enough and will not screen the chemical processes. The conversion profiles of N_2O in the SCR of N_2O by NH_3 on Fe(97)BEAe obtained by the TPSR protocol and steady state conditions are presented in Fig. 5. The N_2O conversion profiles in these two protocols of test superimpose rather nicely. It is noteworthy that in the course of these catalytic tests neither NO nor NO_2 were detected. One should only

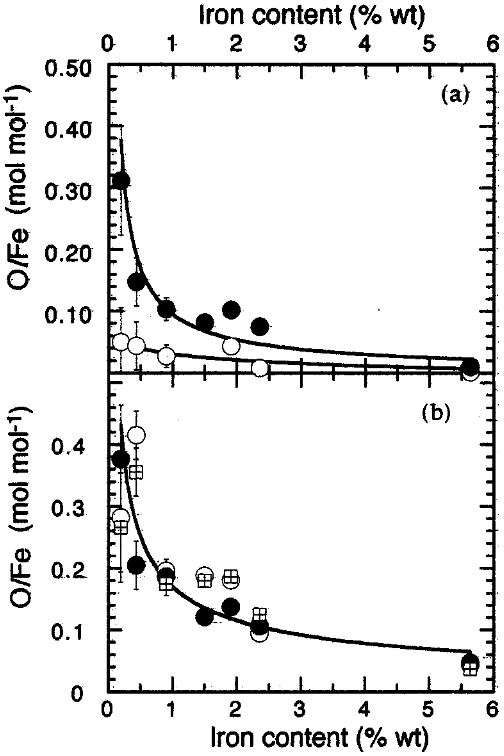

FIG. 4. Amount of O_2 desorbed from Fe-BEA as a function of Fe content, during the O_2-TPD: (a) O/Fe summed in the low temperature region (<700 K); (●) after N_2O treatment of the reduced sample, (○) after N_2O treatment of the calcined sample; (b) O/Fe summed in the high temperature region (>700 K); (●) after N_2O treatment of the reduced sample, (○) after N_2O treatment of the calcined sample, (⊞) after calcination in air.

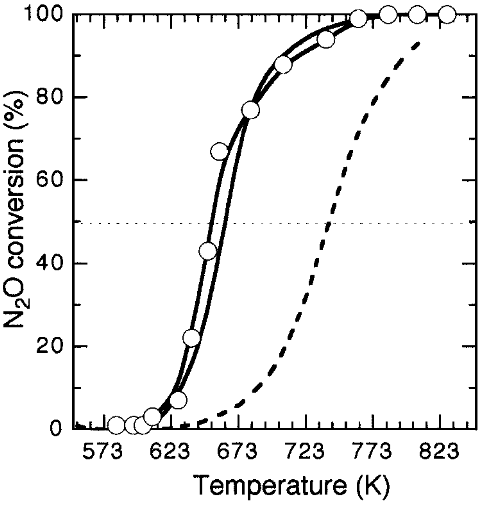

FIG. 5. SCR of N_2O by NH_3 on Fe(97)BEAe as a function of temperature: (——) N_2O conversions obtained in the TPSR protocol (ramp = 10 K min^{-1}, VVH = 35,000 h^{-1}), (—○—) N_2O conversion obtained in steady state experiments by decreasing the temperature from 823 to 573 K by steps of 10–25 K (VVH = 35,000 h^{-1}), (– – –) decomposition of N_2O obtained in the TPSR protocol (ramp = 10 K min^{-1}, VVH = 35,000 h^{-1}).

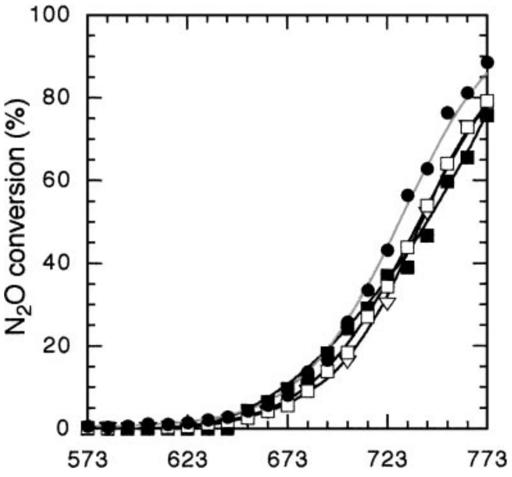

FIG. 6. Catalytic decomposition of N_2O on Fe-BEA catalyst (TPSR protocol, ramp = 10 K min^{-1}, VVH: 35,000 h^{-1}); (—□—) Fe(24)BEAe, (—■—) Fe(49)BEAe, (—▽—) Fe(97)BEAe, (—●—) Fe(126)BEAi.

point out that the N_2O conversions found at steady state conditions are slightly higher than that found in the TPSR experiment in the range 623–678 K. This phenomenon could be due to the strong adsorption of NH_3 and its inhibiting effect on the rate (12) during the ascending ramp of the TPSR; there is a slight delay for NH_3 desorption.

Before discussing the comparative behavior of the various samples for the SCR of N_2O by NH_3, we will briefly present data for the catalytic decomposition on some selected samples calcined in air at 823 K (Fig. 6). The activity of the Fe-free sample was very low. At exchange level $x < 100\%$, the decomposition profiles fall on the same curve, providing evidence that only a small fraction of Fe is actually active. These Fe species are already present at low exchange level ($x \leq 24\%$). Fe-BEA is a very efficient material for N_2O decomposition, where performances are only surpassed by Fe-FER (16), which have been patented catalysts for that reaction (30).

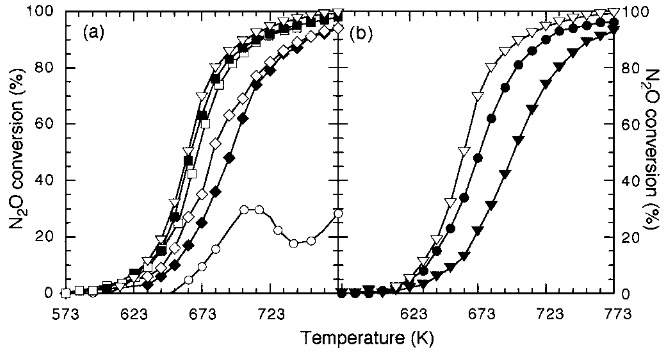

FIG. 7. SCR of N_2O by NH_3 over Fe-BEA catalysts as a function of temperature (TPSR protocol ramp = 10 K min^{-1}, VVH = 35,000 h^{-1}): (—○—) HBEA, (—◆—) Fe(6)BEAe, (—◇—) Fe(10)BEAe, (—□—) Fe(24)BEAe, (—■—) Fe(49)BEAe, (—▽—) Fe(97)BEAe, (—●—) Fe(126)BEAi, (—▼—) Fe(375)BEAi.

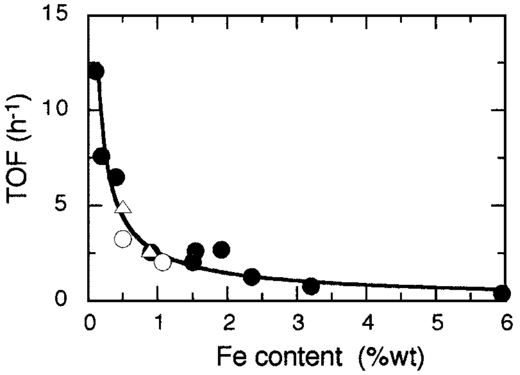

FIG. 8. TOF in the SCR of N_2O by NH_3 as a function of Fe in Fe-BEA catalysts (613 K, steady state conditions of reaction): (—●—) Si/Al = 12.5, (—○—) Si/Al = 25, and (—△—) Si/Al = 39.

The Fe-free H-BEA sample exhibits very low activity for the SCR of N_2O by NH_3 (Fig. 7a). N_2O conversion peaked at 30% for a temperature of ca. 705 K. Upon introduction of a very small amount of iron (0.11% wt, Fe(6)BEAe), as exchanged species to the host BEA, the SCR profile shifts toward low temperature and the conversion increases steadily with temperature. The boosting effect of Fe addition on the light-off temperature for N_2O conversion (50% N_2O conversion) is by ca. 70–90 K. The addition of Fe content up to 97% exchange level intensifies this phenomenon. However, as soon as the exchange level exceeds 100% (Fig. 7b) the SCR profiles are shifted back to higher temperature in comparison to that of Fe(97)BEAe. It is worth noting that Fe(x)BEA is fully composed of iron cationic species at $x < 100$, whereas both cationic species and iron oxide aggregates are present at $x > 100$(25). The activity of iron in SCR can be expressed in terms of turnover frequency (TOF). TOF was calculated from N_2O conversion obtained at steady state conditions and 613 K. The space velocity has been adjusted to maintain the conversion for the various catalysts in the range 10–30%, and the conversion values were taken after 2 h of reaction. At this temperature the secondary reactions, N_2O decomposition and NH_3 oxidation by O_2, only intervene to a very low extent. Figure 8 shows the TOF values as a function of Fe content. The TOF decreases steadily with the Fe content. The TOFs obtained for Fe-BEA prepared from two other H-BEA starting materials, with Si/Al ratios of 25 and 39, fall on the same curve as Fe-BEA prepared from H-BEA with Si/Al ratio of 12.5 (Fig. 8).

DISCUSSION

In the past decade, characterization of iron species in a zeolite host structure has been the subject of numerous works. Several methods of Fe introduction have been developed to exchange specific iron-hydroxo species or to reach high Fe/Al molar ratio (1, 2, 31, 32). In the present work the conventional exchange procedure has been used and the exchange level has been defined as 300 Fe/Al (mol/mol). From a previous study by TPR and Mössbauer spectroscopy of the same materials calcined in air at 823 K (25) we concluded that reducible species are iron-oxo cations in compensation charge of the zeolite up to a theoretical exchange degree close to 100%. As soon as this theoretical exchange degree exceeds 100%, amorphous iron oxide aggregates of small size appear. The proportion of nonreducible Fe species increases with the decrease of the Fe content in the material (see H_2/Fe, Table 1). The nonreducible iron species was considered to be Fe species in tetrahedral coordination in the zeolite lattice. Moreover, near the theoretical exchange of 100% we suggested that Fe would mainly be present as binuclear oxo cations due to H_2/Fe and CO/Fe close to 0.5. The proportion of these species was assumed to decrease with Fe content for statistical reasons. The treatment by N_2O of Fe^{2+}-BEA, obtained from reduction of exchanged and calcined samples, led to the formation of iron-oxo cations with more labile oxygen than after calcination in air (see Fig. 8, Ref. 25) and with an O/Fe_{total} close to 1 for Fe(24)-BEAe. It was proposed that mononuclear iron-oxo cations represent most of the species of N_2O treated Fe(24)-BEAe. At higher Fe content, binuclear iron-oxo cations are also present.

The characterization of these materials by TPD of O_2 reported in the present study strengthens some trends of our previous works (25). Desorption of O_2 from air-calcined materials start above 723 K. If these materials undergo a treatment by N_2O/He (5/95), a small amount of oxygen desorbs at much lower temperatures around 610 K. Therefore this additional treatment favors the formation of new iron-oxo species. This is in agreement with the results of decomposition of N_2O reported above. The desorption of O_2 is the limiting step in the decomposition of N_2O. The temperature at which the decomposition of N_2O ($\approx$623 K) begins is close to the desorption temperature of O_2 from these materials after the air + N_2O pretreatments.

To generate very active Fe-oxo species in higher quantity a reduction by H_2/Ar (3/97) (reduction of Fe^{3+} species to Fe^{2+} species) is necessary before the oxidation by N_2O. With this redox pretreatment the oxygen starts to desorb around 550 K. The SCR of N_2O by NH_3 involves the redox cycle $Fe^{3+} \leftrightarrow Fe^{2+}$ (12). Fe^{3+} initially present in the calcined sample is reduced by NH_3 in Fe^{2+}, which is in turn reoxidized by N_2O. Therefore the catalytic reduction of N_2O will depend on the capacity of the reductant to reduce Fe^{3+} species into Fe^{2+} species. Figure 7a shows that N_2O conversion is observed from 613 K. Taking this into account, it seems that the onset of the SCR of N_2O by NH_3 is determined by the reduction of Fe^{3+} species by NH_3.

In the SCR of N_2O by NH_3, the present study has also shown that (i) fully exchanged Fe(97)-BEAe is the most active catalyst and (ii) the TOF increases when the Fe content decreases. It is immediately apparent that iron oxide aggregates are much less active than exchanged Fe species. Furthermore, if we consider the TOF for Fe-BEA catalysts that only contain Fe exchanged species (wt% Fe < 2) $TOF_{Fe(6)BEAe}$ is 7 times higher than $TOF_{Fe(97)BEAe}$.

In the SCR of NO by NH_3 over Fe-ZSM-5 catalysts, Long and Yang (33) have also observed that the TOF increased with a decreasing iron content with a maximum for Fe/Al = 0.193. These authors underline that acidity plays a positive role in the NO reduction by ammonia, in contrast to the SCR by hydrocarbons. They claimed that the most active Fe-ZSM-5 catalyst exhibits the good balance between Fe and acid sites. As far as Fe-BEA catalysts are concerned, temperature programmed desorption of NH_3 (34) has shown that NH_3 remained adsorbed up to 873 K and no significant difference of desorption profile was observed at various Fe content. We have also ascertained that Fe-BEA of similar Fe content but prepared from BEA of different Si/Al ratios exhibit comparable TOF (Fig. 8). In these materials the amounts of remaining protons are very likely different. These facts prompt us to think that the higher TOF at low exchange does not result from a better balance with acid sites but rather from the occurrence in higher proportion of much more active Fe species.

Panov *et al.* (19) have proposed that N_2O interacts selectively with specific Fe sites of Fe-ZSM-5 to give adsorbed O^* (the so-called α-oxygen), which is highly active in the oxidation of benzene to phenol. From several studies (Ref. 19 and references therein) Panov's group has deduced that these iron sites are isolated ions or small complexes inside the intracrystalline micropore space of the ZSM-5 matrix. Moreover, they have suggested that α-sites are most probably associated with binuclear Fe-oxo complexes rather than with single Fe atoms. From *ab initio* quantum chemical calculations, Arbuznikov and Zhidomirov (35) confirmed the probability of similar binuclear oxo cations with peroxide bridges and hydroxyl groups. Lazar *et al.* (36, 37) also proposed an oxygen bridge between two Fe atoms, one of the two belonging to the zeolite framework. The main problem associated with these models of a binuclear complex is their probability of occurrence, which should decrease as the Fe content decreases too.

In this work we have found that the TOF is high on Fe(24)-BEAe, which mainly contains monuclear oxo cations after the redox pretreatment by H_2, followed by N_2O (25). Very reactive isolated Fe^{3+} species in a distorted tetrahedral environment have also been proposed to activate easily N_2O on Fe-ZSM-5 (38). However, we have found that Fe in tetrahedral substitution of Al in [Fe]-BEA is much less active than Fe-exchanged BEA (34). From DFT computations, Yoshizawa *et al.* (39) proposed that "α-O" has relevance to mononuclear iron-oxo species of the type $(FeO)^+$ on a AlO_4 surface site of a ZSM-5 zeolite. It is clear that the debate about the exact nature of the mononuclear Fe-oxo cation remains open. Moreover, the BEA framework is very flexible, allowing (i) reversible changes from tetrahedral to octahedral coordination of Al (40) and (ii) the presence of defects, dangling bonds, and partially coordinated aluminic fragments. We can only propose that isolated mononuclear Fe sites are very likely the most active species in Fe-BEA for the SCR of N_2O by NH_3 in the presence of O_2. This is due to the higher lability of adsorbed O^* formed from the interaction of N_2O with these sites (Fig. 4a). From O_2-TPD (Fig. 4), H_2-TPR, and CO-TPR (26), binuclear Fe-oxo cations coexist with mononuclear species at full exchange level ($\approx$2 wt% Fe). From the plot of TOF as a function of Fe content (Fig. 8), it is clear that binuclear species are less active than the mononuclear species.

CONCLUSIONS

Oxygen lability of iron-oxo cations in charge compensation of Fe-BEA catalysts with different iron content has been investigated. We have shown the importance of reducing Fe-BEA to Fe^{2+}-BEA before the N_2O reoxidation step. This whole pretreatment induces specific formation of iron-oxo species with an oxygen lability greatly enhanced in comparison to samples without any reducing step pretreatment. In the SCR of N_2O by NH_3 the specific activity increases with the iron exchange level up to 100%. The comparison of the specific activities at 613 K expressed by mole of iron (TOF) has clearly shown the presence of high reactive Fe sites, which are predominantly present in the Fe-BEA catalysts with low iron content. Mononuclear iron-oxo cations have been proposed as the highest reactive sites for the reduction of N_2O by NH_3; binuclear iron-oxo species and iron oxides aggregates are less active.

ACKNOWLEDGMENT

M.M. warmly thanks the Ministère Français de l’Education Nationale, de la Recherche et de la Technologie for a scholarship.

REFERENCES

1. Chen, H. Y., and Sachtler, W. M. H., *Catal. Today* **42**, 73 (1998).
2. Feng, X. B., and Hall, W. K., *J. Catal.* **166**, 368 (1997).
3. Joyner, R., and Stockenhuber, M., *J. Phys. Chem. B* **103**, 5963 (1999).
4. Lee, H. T., and Rhee, H. K., *Catal. Lett.* **61**, 71 (1999).
5. Lobree, L. J., Hwang, I. C., Reimer, J. A., and Bell, A. T., *Catal. Lett.* **63**, 233 (1999).
6. Lombardo, E. A., Sill, G. A., d’Itri, J. L., and Hall, W. K., *J. Catal.* **173**, 440 (1998).
7. Long, R. Q., and Yang, R. T., *J. Am. Chem. Soc.* **121**, 5595 (1999).
8. Ma, A. Z., and Grunert, W., *Chem. Commun.* 71 (1999).
9. Butchart, N., Austin, J., Knight, J. R., Scaife, A. A., and Gallani, M. L., *J. Climate* **13**, 2142 (2000).
10. Kapteijn, F., Rodriguez-Mirasol, J., and Moulijn, J. A., *Appl. Catal. B* **9**, 25 (1996).
11. Centi, G., and Vazzana, F., *Catal. Today* **53**, 683 (1999).
12. Coq, B., Mauvezin, M., Delahay, G., and Kieger, S., *J. Catal.* **195**, 298 (2000).
13. Kameoka, S., Suzuki, T., Yuzaki, K., Takeda, T., Tanaka, S., Ito, S., Miyadera, T., and Kunimori, K., *Chem. Commun.* 745 (2000).
14. Pophal, C., Yogo, T., Tanabe, K., and Segawa, K., *Catal. Lett.* **44**, 271 (1997).
15. Yamada, K., Kondo, S., and Segawa, K., *Microporous Mesoporous Mater.* **35–36**, 227 (2000).
16. Mauvezin, M., Delahay, G., Kießlich, F., Coq, B., and Kieger, S., *Catal. Lett.* **62**, 41 (1999).
17. Pophal, C., Yogo, T., Yamada, K., and Segawa, K., *Appl. Catal. B* **16**, 177 (1998).
18. Ovanesyan, N. S., Shteinman, A. A., Dubkov, K. A., Sobolev, V. I., and Panov, G. I., *Kinet. Catal.—Engl. Tr.* **39**, 792 (1998).
19. Panov, G. I., Uriarte, A. K., Rodkin, M. A., and Sobolev, V. I., *Catal. Today* **41**, 365 (1998).
20. Volodin, A. M., Sobolev, V. I., and Zhidomirov, G. M., *Kinet. Catal.—Engl. Tr.* **39**, 775 (1998).
21. Battiston, A. A., Bitter, J. H., and Koningsberger, D. C., *Catal. Lett.* **66**, 75 (2000).
22. Lobree, L. J., Hwang, I. C., Reimer, J. A., and Bell, A. T., *J. Catal.* **186**, 242 (1999).
23. Marturano, P., Drozdova, L., Kogelbauer, A., and Prins, R., *J. Catal.* **192**, 236 (2000).
24. Voskoboinikov, T. V., Chen, H. Y., and Sachtler, W. M. H., *Appl. Catal. B* **19**, 279 (1998).
25. Mauvezin, M., Delahay, G., Coq, B., Kieger, S., Jumas J. C., and Olivier-Fourcade J., *J. Phys. Chem. B* **105**, 928 (2001).
26. Inamura, K., Iwamoto, R., Iino, A., and Takyu, T., *J. Catal.* **142**, 274 (1993).
27. Mahoney, F., Rudham, R., and Summers, J. V., *J. Chem. Soc. Faraday Trans. 1* **75**, 314 (1979).
28. El Malki, E. M., van Santen, R. A., and Sachtler, W. M. H., *J. Catal.* **196**, 235 (2000).
29. Grubert, G., Hudson, M. J., Joyner, R. W., and Stockenhuber, M., *J. Catal.* **196**, 126 (2000).
30. Neveu, B., Hamon, C., and Malefant, K., World Intellectual Property Organization (WIPO) patent: WO9934901A1, 1999.
31. Delgass, W. N., Garten, R. L., and Boudart, M., *J. Chem. Phys.* **50**, 4603 (1969).
32. Kogel, M., Sandoval, V. H., Schwieger, W., Tissler, A., and Turek, T., *Catal. Lett.* **51**, 23 (1998).
33. Long, R. Q., and Yang, R. T., *J. Catal.* **188**, 332 (1999).
34. Mauvezin, M., Ph.D. dissertation, Montpellier, France, 2000.
35. Arbuznikov, A. V., and Zhidomirov, G. M., *Catal. Lett.* **40**, 17 (1996).
36. Lazar, K., Kotasthane, A. N., and Fejes, P., *Catal. Lett.* **57**, 171 (1999).
37. Lazar, K., Lejeune, G., Ahedi, R. K., Shevade, S. S., and Kotasthane, A. N., *J. Phys. Chem. B* **102**, 4865 (1998).
38. Ribera, A., Arends, I. W. C. E., de Vries, S., Pérez-Ramírez, J., and Sheldon, R. A., *J. Catal.* **195**, 287 (2000).
39. Yoshizawa, K., Yumura, T., Shiota, Y., and Yamabe, T., *Bull. Chem. Soc. Jpn.* **73**, 29 (2000).
40. Bourgeat-Lami, E., Massiani, P., Di Renzo, F., Espiau, P., Fajula, F., and des Courières, T., *Appl. Catal.* **72**, 139 (1991).